Effect of Magnetic and Electric Fields on Synthesis of Cu Nanoparticles by Laser Ablation Method and Investigation of their Structural Properties

Mahdieh Razaghianpour
mohammad reza hantehzadeh (hantehzadeh@hotmail.com)
Amir Hossein Sari
Elham Darabi

Research Article

Keywords: Copper nanoparticles, Laser ablation, Magnetic field, Electric Field

Posted Date: March 3rd, 2022

DOI: https://doi.org/10.21203/rs.3.rs-1409427/v1

Abstract

In this study, copper nanoparticles were synthesized and identified by laser ablation method. For the synthesis of copper nanoparticles, a constant magnetic field equal to 10 mT and different electric fields equal to 0, 10, 15, 20 and 25 V/Cm were applied and their effect on the properties and morphology of the nanoparticles were investigated. The synthesized nanoparticles were characterized using XRD, FTIR, RAMAN, UV–Vis spectrum, FE-SEM and TEM analyzes. The results of UV–Vis spectrum indicated that the size of nanoparticles was decreased by increasing the applied electric field. RAMAN and XRD analysis showed that the amount of copper nanoparticles were increased with increasing the applied electric field and also FTIR analysis confirmed that copper nanoparticles were formed. The FESEM images showed that with increasing electric field along with constant magnetic field, nanoparticles from spherical to flower-shaped and to rod-like were formed. The purity of the synthesized copper nanoparticles was confirmed by EDX spectra. TEM images of the nanoparticles showed that by increasing the electric field, the crystalline form of the nanoparticles shifted from large scales spherical particles to rod-like nanoparticles and then transformed to rod-like with very small spherical particles.

1. Introduction

The excellent properties and various applications of metal nanoparticles make these nanoparticles widely used in many industries including energy, catalysis, environment, semiconductors and medicine, that to be given more attention by researchers [1, 2]. Among the various noble metal nanoparticles, copper based nanoparticles (copper, copper oxide and cuprous oxide) have received a lot of attention because of their many physico-chemical properties such as mechanical, optical, electrical and low cost [3–5]. These interesting and unique properties of copper have led to many applications in architectures, auto-motives, bio-medicals, solar cells, sensors, catalysis, optoelectronics and etc [6, 7]. Copper-based nanoparticles are synthesized by a variety of chemical and physical methods such as chemical precipitation, sol-gel, sonochemical, hydrothermal, electrochemical, photochemical, biological method, mechanical-ball milling, pulse laser ablation, micro-emulsion, thermal decomposition, microwave synthesis method and etc [8, 9, 18–22, 10–17].

Among the various synthesis methods, pulse laser ablation method in liquids is a unique technique for fabricating the nanoparticles. Laser ablation is an easy, simple, fast and laboratory safe method for synthesis of nanopraticles. On the other hand, because the laser ablation method is performed without the use of any surfactants, other chemical agents and toxic, hazardous chemical precursors for fabricating of nanoparticles, and thus is considered a green and environmentally friendly method, which is an advantage compared to other methods. Also in this method, the shape, morphology and size of the particles can be controlled by controlling the applied laser pulse [23–26]. The properties of synthesized nanopraticles for a variety of applications in different industries depended greatly on the shape, structure and size of the nanoparticles. Therefore, controlling the shape, size and structure were of great importance during in the synthesis process. Recent research demonstrated that the applied of external fields (such as magnetic field and electric field) could be a great effect in controlling the shape and size

of particles in laser ablation method. Therefore, in this study, the external field was used in laser ablation method and their effect on the size, shape and properties of copper nanoparticles was investigated.

The aim of this study, the synthesis of copper nanoparticles by laser ablation method in the presence of a constant magnetic field and different electric fields. Also, the structure, morphology and properties of nanoparticles synthesized under different conditions were studied by using XRD, FTIR, RAMAN, UV–Vis spectrum, FE-SEM and TEM analyzes.

2. Experimental

2.1. Laser Ablation

The schematic of the laser ablation setup for the synthesis of nanoparticles is shown in Fig. 1. For the synthesis of Cu nanoparticles, first the copper plate (10*10 mm^2) was placed under ultrasonic waves in ethanol, acetone and distilled water bath, respectively, to clean the copper surface and be free of any impurities. Then, the copper target was immersed in distilled water and the laser waves with a wavelength of 1064 nm were irradiated by a pulsed Nd:YAG laser source. To investigate the effect of electric field on the synthesis of copper nanoparticles, voltage was applied to two 2.6*2 cm^2 gold electrodes immersed in distilled water. Fluence of the laser pulse in the nanoparticle synthesis process was estimated by energy meter from Spectrum Laser Inc. A cubic magnet was placed under the bottom of the reaction vessel to apply a constant magnetic field equal to 10 mT. Intensity of the magnetic field was estimated by a Gaussmeter (Leybold didactic GMBH). Second, to apply different electrical potentials of 0, 20, 30, 40 and 50 volts (or different electric fields equal to 0, 10, 15, 20 and 25 V/Cm) on plates and electric fields related to these electric potentials, i.e. 0 V/cm, 10 V/cm, 15 V/cm, 20 V/cm and 25 V/cm were created. During the laser ablation process for the synthesis of copper nanoparticles, the temperature of water was 25°C and the time of applied voltage for each sample was 7 minutes. After the laser ablation process, nanoparticles were collected and analyzed.

2.2. Characterization Technics

X-ray diffraction (XRD) data was collected by d8-Burker system. Transmission electron microscopy (TEM) image was taken using ZEISS EM 10C TEM with an accelerating voltage of 100 kV. The field emission scanning electron microscopy (FE-SEM) images and energy dispersive X-ray (EDX) spectra were taken on a JEOL JSM 6390 LV scanning electron microscope. Infrared absorption data were obtained by using a Fourier-transform-infrared (FT-IR) spectrometer TENZOR 27 (Bruker, Germany). Raman spectra were recorded with LabRam ARAMIS (HORIBA Jobin-Yvon) system using the exciting line at 532nm of He-Ne laser. Dynamic light scattering (DLS) analysis was measured using a Zetasizer Nano ZS90 instrument (Malvern, UK). UV-Vis spectra were measured with a Varian Cary 500 scan UV-Vis NIR spectrophotometer in the range of 200–800nm with 1cm path length quartz cuvettes.

3. Results And Discussion:

3.1 XRD analysis:

The XRD pattern of synthesized samples (No. a, b, c, d and f) in different conditions summarized in Fig. 2. As can be seen from the XRD patterns, at 0V the most cuprous oxide (Cu_2O) nanoparticles are present, which is related to diffraction at peak at about 2θ = 36.52º (JCPDS No. 01-077-0199), and a small amount of copper (Cu) nanoparticles, which is related to diffraction at peak at about 2θ = 43.47º. But by applying an electrical field, copper nanoparticles began to form. The diffraction peak at about 2θ = 43.47º, 50.37º and 73.95º which match with the (111), (200) and (220) Miller indices of copper by increases the electrical field are clearly appeared. The corresponding crystal structure of copper nanoparticles for these diffraction peaks was cubic with Fm-3m space group (JCPDS No. 00-001-1241). The results show The XRD results displayed the presence of both Cu and Cu_2O in the all the synthesized samples of nanoparticles. The presence of Cu_2O nanoparticles can be related to the oxidation of copper in water during the synthesis process. The crystalline size of samples were estimated by the diffraction peak at about 2θ = 43.47º with using well-known Scherrer equation [27]. The calculated results show that the crystalline size of samples were found to be around 17.1 nm (0V), 14.2 nm (20V), 12.1 nm (30V), 10.7 nm (40V) and 10.9 nm (50V).

3.2. FT-IR spectroscopy:

The FT-IR spectroscopy of samples were depicted in Fig. 3 that was useful technique to identify functional groups. The peak at about 3450 cm^{-1} in all samples shows the presence of OH functional groups. Also, the peak at about 1630 cm^{-1} ascribed to the bending mode of the adsorbed water on the nanoparticle. The peak at about 480 and 620 cm^{-1} corresponded to the metal and metal oxide bond (Cu and Cu-O) [28–30]. As seen in results of Fig. 3, the metal and metal oxide signal was appeared that confirmed the synthesis of nanoparticles.

3.3. UV–Vis spectrum:

The UV–Vis absorbance spectra of samples synthesized in different voltage are illustrated in Fig. 4. In order to evaluate the optical properties of the synthesized nanoparticles, the absorbance of each sample was measured in the range of 200–800 nm by UV-visible spectroscopy. In all the obtained samples, two intense peaks observed at about ~270 and ~570 nm. The peaks at about ~570 nm for all samples were related to the surface plasmon resonance (SPR) of Cu nanoparticles. Another absorption peaks for all samples have appeared at about ~270 nm were caused from the Brillouin transitions of cuprous oxide (Cu_2O). The observed slight blue shift by increasing applied electric field from 0 to 50 volts, can be attributed to the average size of nanoparticles were decreased [31, 32].

3.4. RAMAN analysis

RAMAN spectroscopy has excellent application for chemical recognition of noble metals as copper, gold or silver on nanostructured surfaces. Colloidal metals have high nanostructured surface that provides strong RAMAN enhancements. As Fig. 5 shows, RAMAN scattering experiment of obtained nanoparticles at 0V, shows that Cu_2O peaks appeared at 76.53 and 252.11 cm^{-1} and the characteristic peaks at 407.94, 1447.96 and 1772.20 are related to Cu nanoparticles. For obtained nanoparticles in 20V, the observed RAMAN peaks of Cu_2O phase are at 87.04 and 636.67 cm^{-1} and 409.16, 1452.83 and 1772.20 cm^{-1} are the fingerprints of Cu nanoparticles. In 30V, peaks in RAMAN are at 85.72 and 632.51 cm^{-1} correspond to Cu_2O and Cu nanoparticles peaks appeared at 409.16 and 1448.93 cm^{-1}. In an electric field equal to 40V, the RAMAN spectrum shows two peaks at 87.04 and 688 cm^{-1} of Cu_2O with two distinct peaks at 409.16 and 1447.96 cm^{-1} corresponding to Cu nanoparticles. In the RAMAN spectrum of obtained nanoparticles at 50V the characteristic peaks at 84.69 and 604.49 cm^{-1} corresponds to Cu_2O and 407.94 and 1446.01 cm^{-1} are related to Cu nanoparticles [32–34]. The mechanism of oxidation of Cu nanoparticles is complex but as above-reported shows that by synthesizing copper nanoparticles by laser ablation in water, some copper oxide is also synthesized with it.

3.5. Scanning electron microscope analysis

The FE-SEM images with corresponding EDS spectrum maps are summarized in Fig. 6. As can be seen from the FE-SEM images, the surface morphology of the synthesized nanoparticles has changed with increasing electric field. First, without applying electrical potentials (0 volt), particles were mostly seen as agglomerated with large size of scale. Afterward, by applying an electric field, the surface morphology of the nanoparticles changed, which formed a spherical shaped in a 20-volt electrical potentials. In an electrical potentials equal to 30 volts, the particles formed in flower-shaped surface morphology. On the other hand, nanoparticles were synthesized as rod-shape morphology by increasing the electrical potentials to 40 volts which seems to be formed from the aggregation of very small spherical particle. Eventually, by increasing the electrical potentials to 50 volts, spherical agglomerated nanoparticles were formed. The EDS spectrum maps samples are also shown in Fig. 7. The EDS spectra of the samples clearly indicate that highly pure copper nanoparticles and without any impurity were formed.

3.6. Transmission electron microscopy analysis

The TEM images were used to identify the crystal morphology of the synthesized samples, as shown in Fig. 8. TEM images of samples synthesized without an applied electric field or electrical potentials (0 volt) show that the nanoparticles formed in spherical-like nanoflakes. By increased the applied electrical potentials (20 volts) nanoparticles formed in spherical shape. Afterward, by increasing the electrical potentials to 30 volts the particles formed in flower and rod-like shaped. In an electrical potentials equal to 40 volts, show the unusual crystal morphology compared to surface morphology of particles which confirmed with SEM images. On the other hand, it appears that numerous primary small nanoparticles roughly 7–9 nm interconnected with one another to form larger secondary rod-like architectures with hollow boundaries by definite border between the small components. Then, by increasing applied

electrical potentials to 50 volts, TEM image indicated that the crystal morphology of particles was a combination of spherical and rod-like nanoparticles. Also, the colloids prepared as monodisperse copper nanoparticles were measured using dynamic light scattering (DLS) analysis. The DLS analysis was used to confirm the particle size distribution. The DLS data (Fig. 9(a)) show that the Z-average size of nanoparticles synthesized at 25 V/cm was 156.3nm. On the other hand, the presence of a peak indicated the high quality of copper nanoparticles. Also, the Zeta potential of the synthesized Cu nanoparticles in the colloidal solution was presented in Fig. 9(b), which obtained 25.1mV.

4. Conclusions

Copper nanoparticles were synthesized by laser ablation method and under a constant magnetic field of 10 mT and different electrical potentials of 0, 20, 30, 40 and 50 volts. The results showed that with increasing electric field, the amount of synthesized copper nanoparticles have increased. Also, the XRD and UV–Vis spectrum obtained results indicated that the crystalline size of copper nanoparticles became smaller with increasing applied electric field. On the other hand, because the synthesis process with laser ablation was in water, some copper oxide was also synthesized. The FE-SEM and TEM images clearly showed that with increasing applied electric field, the morphology of the synthesized nanoparticles changed, so that with increasing electric field, the nanoparticles changed from spherical to rod-like shaped morphology that was clearly observed by TEM images.

Declarations

The Authors declare that there is no conflict of interest.

References

1. N. Kulkarni and U. Muddapur, J. Nanotechnol. **2014**, (2014).
2. C. N. R. Rao, G. U. Kulkarni, P. J. Thomas, and P. P. Edwards, Chem. Soc. Rev. **29**, 27 (2000).
3. T. Pradeep and Anshup, Thin Solid Films **517**, 6441 (2009).
4. Liu P, Wang H, Li X, Rui M, Zeng H. Rsc Adv. 5, 79738 (2015).
5. V. Pareek, A. Bhargava, R. Gupta, N. Jain, and J. Panwar, Adv. Sci. Eng. Med. **9**, 527 (2017).
6. P. K. Khanna, S. Gaikwad, P. V. Adhyapak, N. Singh, and R. Marimuthu, Mater. Lett. **61**, 4711 (2007).
7. N. A. Dhas, C. P. Raj, and A. Gedanken, Chem. Mater. **10**, 1446 (1998).
8. X. Zhu, B. Wang, F. Shi, and J. Nie, Langmuir **28**, 14461 (2012).
9. J. N. Solanki, R. Sengupta, and Z. V. P. Murthy, Solid State Sci. **12**, 1560 (2010).
10. M. Salavati-Niasari, F. Davar, and N. Mir, Polyhedron **27**, 3514 (2008).
11. S. Mirsafai, K. Torabi, M. Ashrafi, and M. Hamadanian, Bull. Mater. Sci **43**, 101 (2034).
12. B. Khodashenas and H. R. Ghorbani, Korean J. Chem. Eng. **31**, 1105 (2014).
13. L. Huang, H. Jiang, J. Zhang, Z. Zhang, and P. Zhang, Electrochem. Commun. **8**, 262 (2006).

14. C. H. Han and B. G. Min, Fibers Polym. **21**, 785 (2020).
15. V. S. Gurin, A. A. Alexeenko, S. A. Zolotovskaya, and K. V. Yumashev, Mater. Sci. Eng. C **26**, 952 (2006).
16. D. A. Goncharova, T. S. Kharlamova, I. N. Lapin, and V. A. Svetlichnyi, J. Phys. Chem. C **123**, 21731 (2019).
17. M. F. El-Berry, S. A. Sadeek, A. M. Abdalla, and M. Y. Nassar, Mater. Res. Bull. **133**, 111048 (2021).
18. Z. Dashtizadeh, F. Jookar Kashi, and M. Ashrafi, Mater. Today Commun. **27**, 102456 (2021).
19. M. Ashrafi, M. Hamadanian, A. R. Ghasemi, and F. J. Kashi, Polym. Compos. **40**, 3393 (2019).
20. B. Ashok, N. Hariram, S. Siengchin, and A. V. Rajulu, J. Bioresour. Bioprod. **5**, 180 (2020).
21. S. U. Din, J. M. Awan, M. Imran, Zain-Ul-Abdin, S. Haq, M. Hafeez, S. Hussain, and M. S. Khan, Microsc. Res. Tech. (2021).
22. V. Dalouji, S. Goudarzi, and S. Solaymani, Microsc. Res. Tech. **84**, 1205 (2021).
23. N. G. Semaltianos, Crit. Rev. Solid State Mater. Sci. **35**, 105 (2010).
24. Zhang D, Li Z, Sugioka K. JPhys Photonics. (2021) https://doi.org/10.1088/2515-7647/ac0bfd.
25. H. L. Aye, S. Choopun, and T. Chairuangsri, in Adv. Mater. Res. (Trans Tech Publications Ltd, 2010), pp. 83–86.
26. M. Bakhtiari, M. Hantehzadeh, and E. Darabi, Microsc. Res. Tech. (2021).
27. A. F. Zonouz, M. Ashrafi, M. Ghiyasiyan-Arani, and M. Hamadanian, J. Elastomers Plast. **53**, 241 (2021).
28. M. Nasrollahzadeh, M. Atarod, and S. M. Sajadi, J. Colloid Interface Sci. **486**, 153 (2017).
29. S. Nazari, H. Safarzadeh, and M. Bahiraei, J. Clean. Prod. **208**, 1041 (2019).
30. M. A. Bhosale and B. M. Bhanage, RSC Adv. **4**, 15122 (2014).
31. A. H. M. Al-Antaki, X. Luo, X. Duan, R. N. Lamb, W. D. Hutchison, W. Lawrance, and C. L. Raston, ACS Omega **4**, 13577 (2019).
32. H. Dizajghorbani Aghdam, H. Azadi, M. Esmaeilzadeh, S. Moemen Bellah, and R. Malekfar, Opt. Mater. (Amst). **91**, 433 (2019).
33. P. K. Baruah, A. K. Sharma, and A. Khare, Opt. Laser Technol. **108**, 574 (2018).
34. H. J. Jung and M. Y. Choi, (2015).

Figures

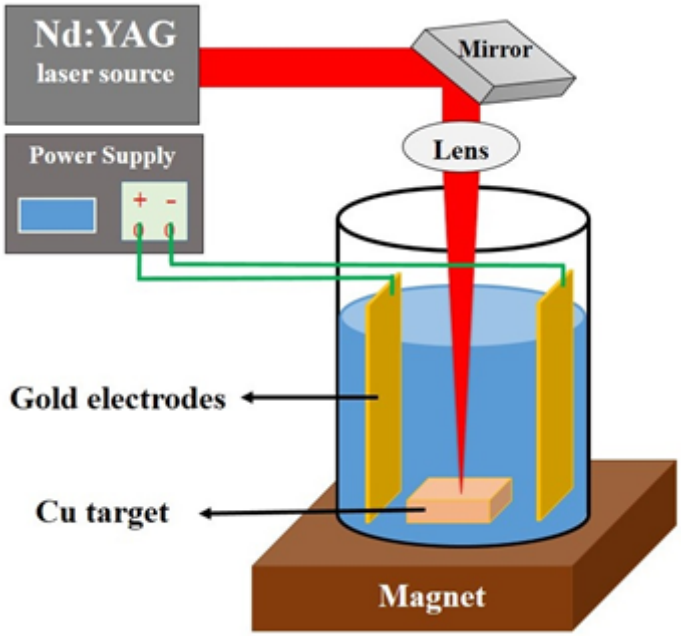

Figure 1

Schematic of the laser ablation setup for the synthesis of Cu nanoparticles

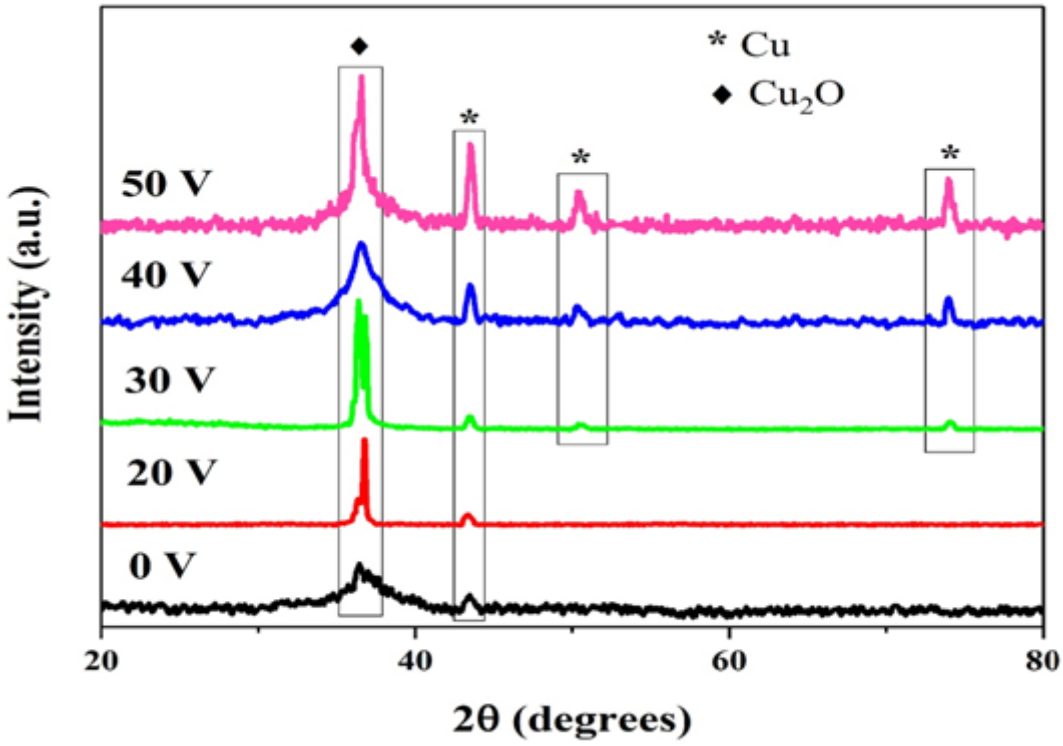

Figure 2

XRD pattern of Cu nanoparticles in constant magnetic field (10 mT) and different electrical potentials

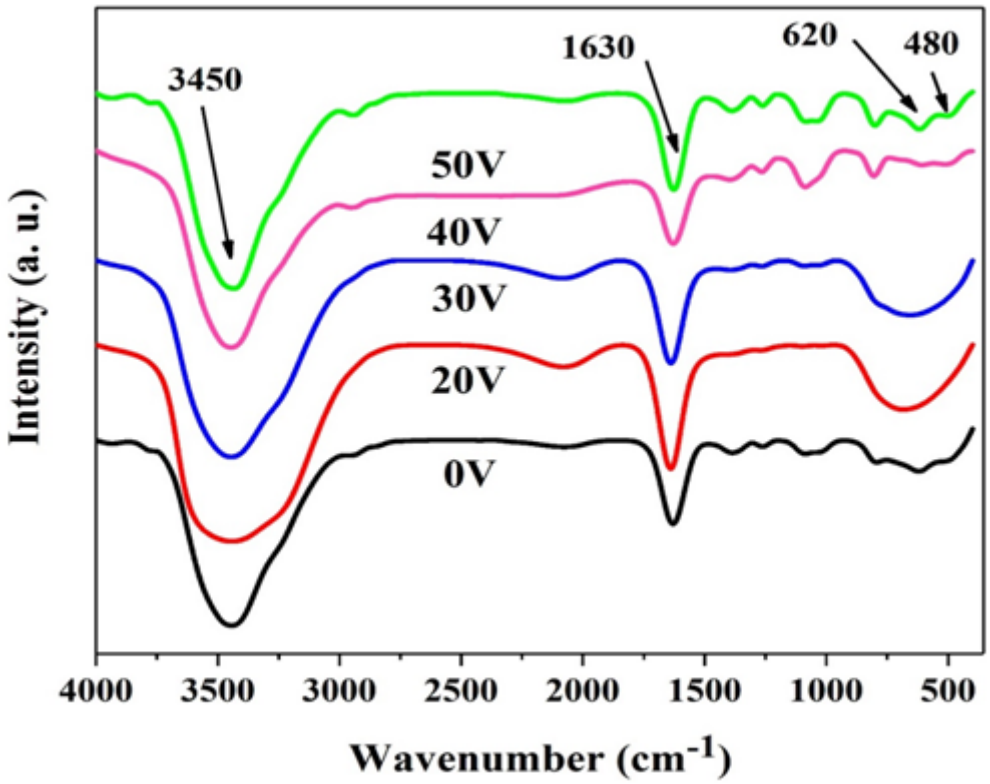

Figure 3

FT-IR spectroscopy of Cu nanoparticles in constant magnetic field (10 mT) and different electrical potentials

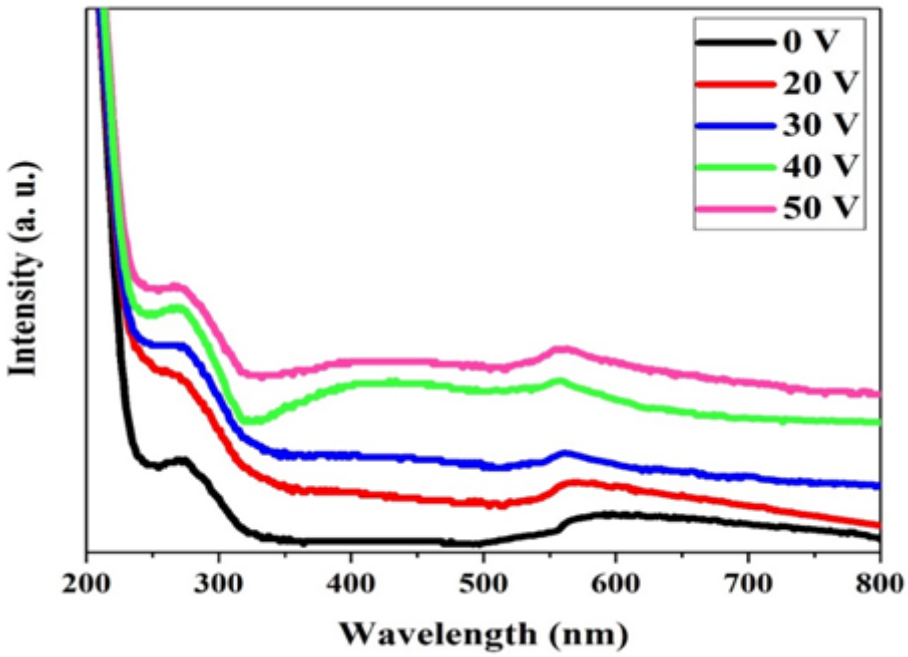

Figure 4

UV–Vis absorbance spectra of Cu nanoparticles in constant magnetic field (10 mT) and different electrical potentials

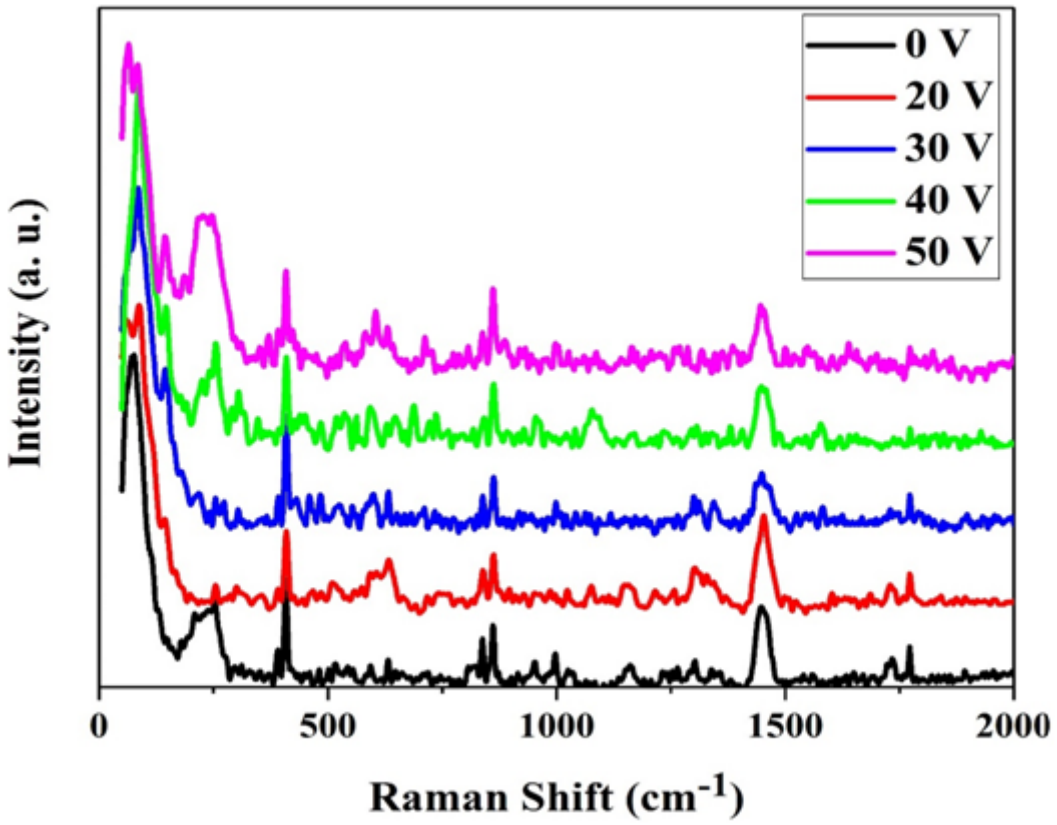

Figure 5

RAMAN spectra of Cu nanoparticles in constant magnetic field (10 mT) and different electrical potentials

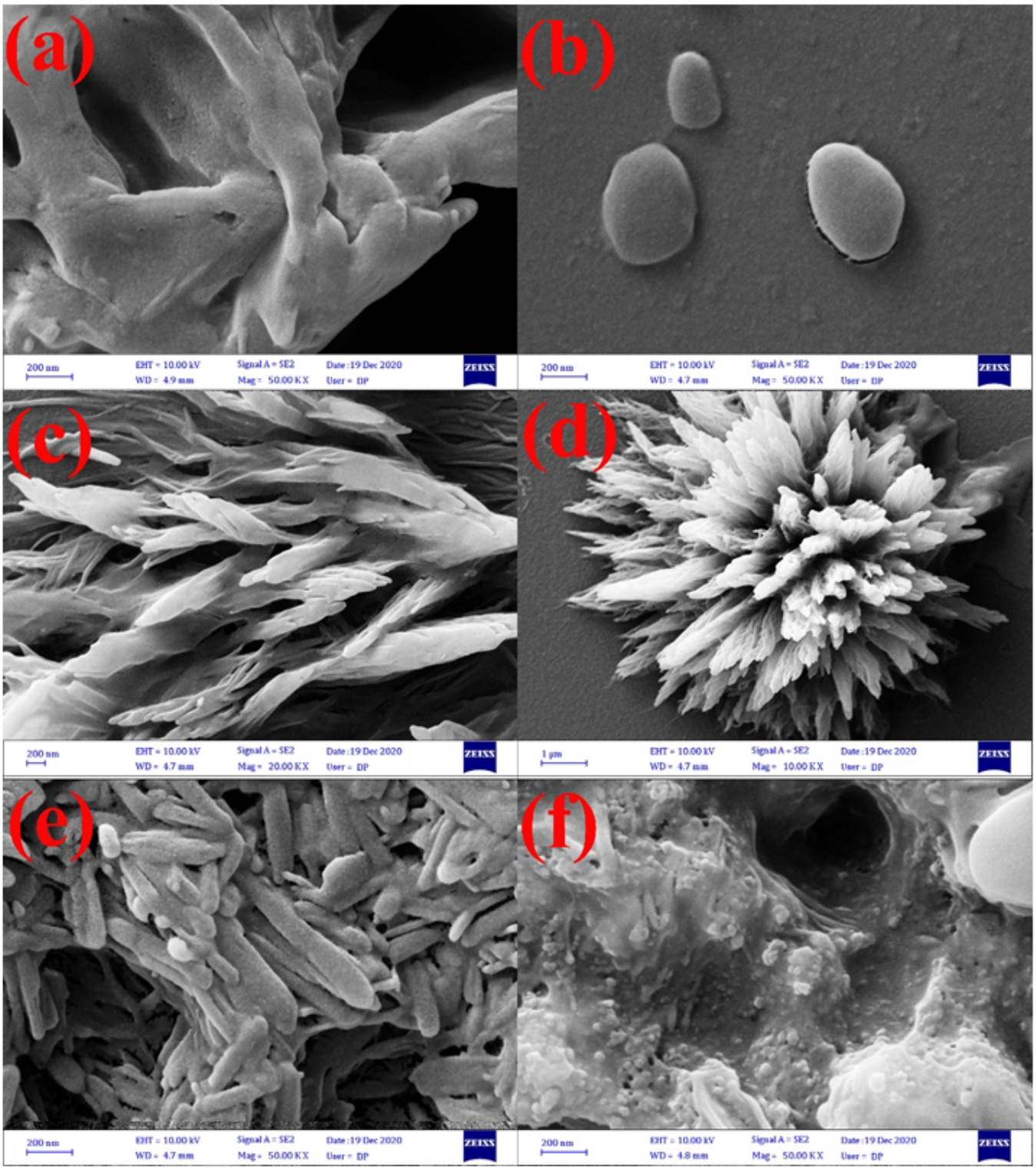

Figure 6

FESEM images of Cu nanoparticles in constant magnetic field (10 mT) and different electrical potentials equal to 0 (a), 20 (b), 30 (c and d), 40 (e) and 50 (f) volts

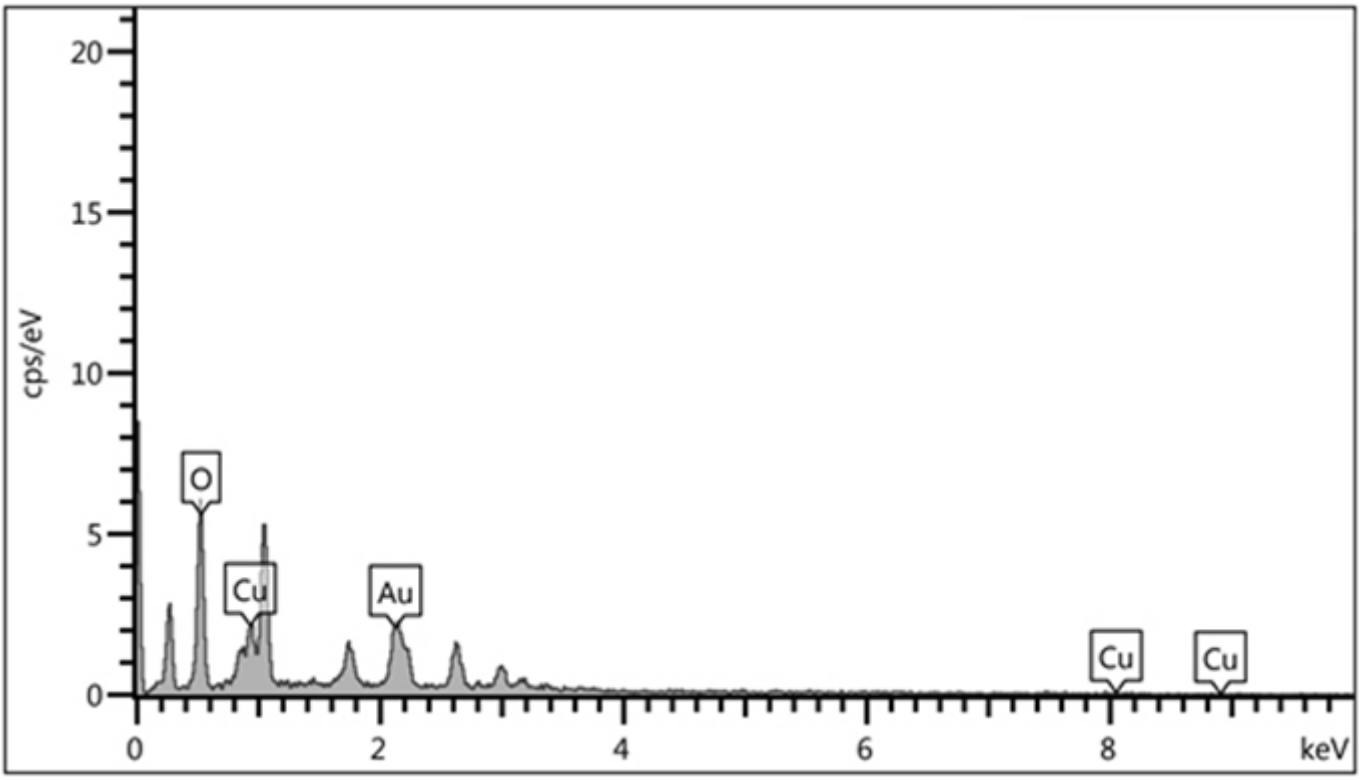

Figure 7

The EDS spectrum of Cu nanoparticles

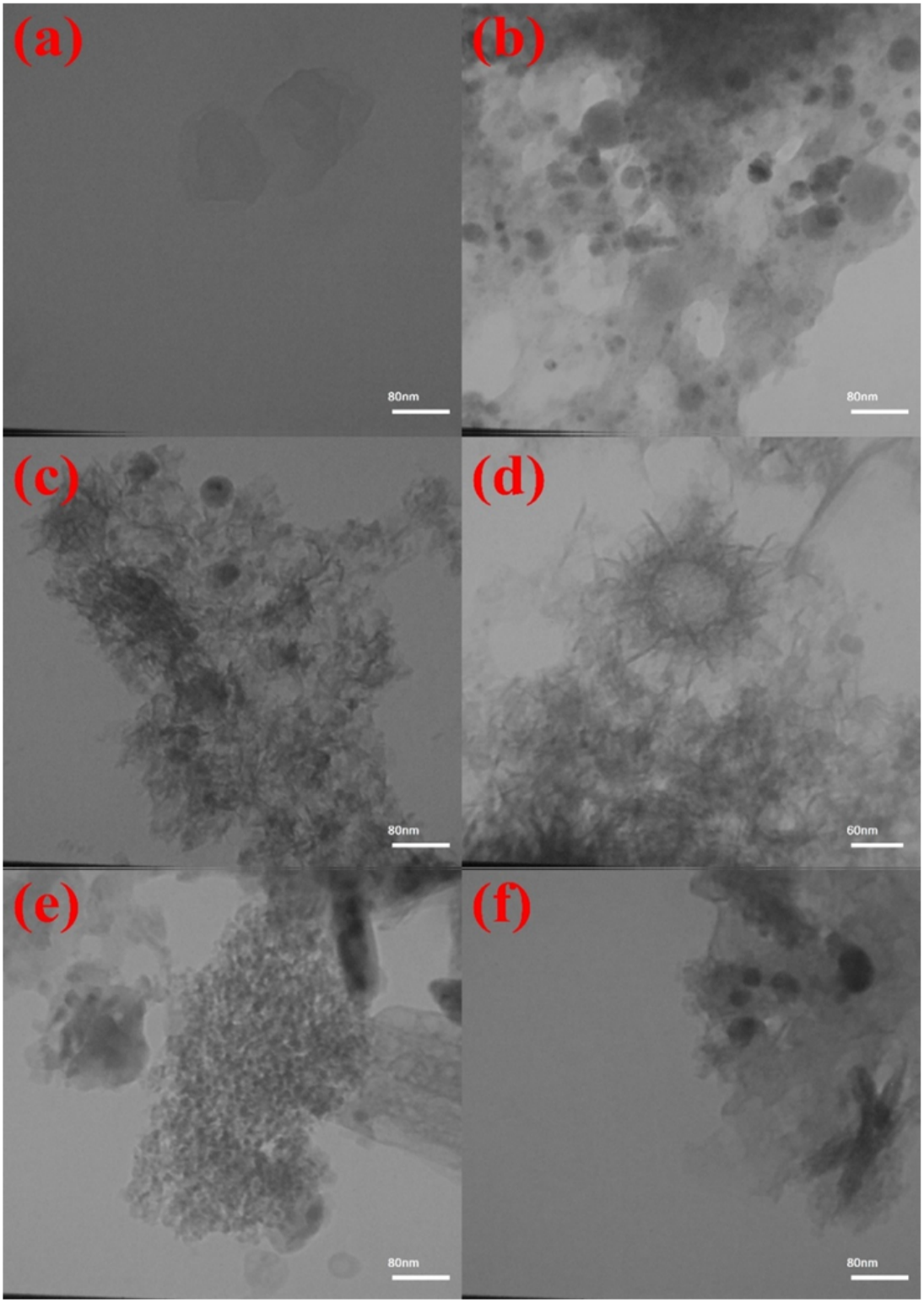

Figure 8

TEM images of Cu nanoparticles in constant magnetic field (10 mT) and different electrical potentials equal to 0 (a), 20 (b), 30 (c and d), 40 (e) and 50 (f) volts

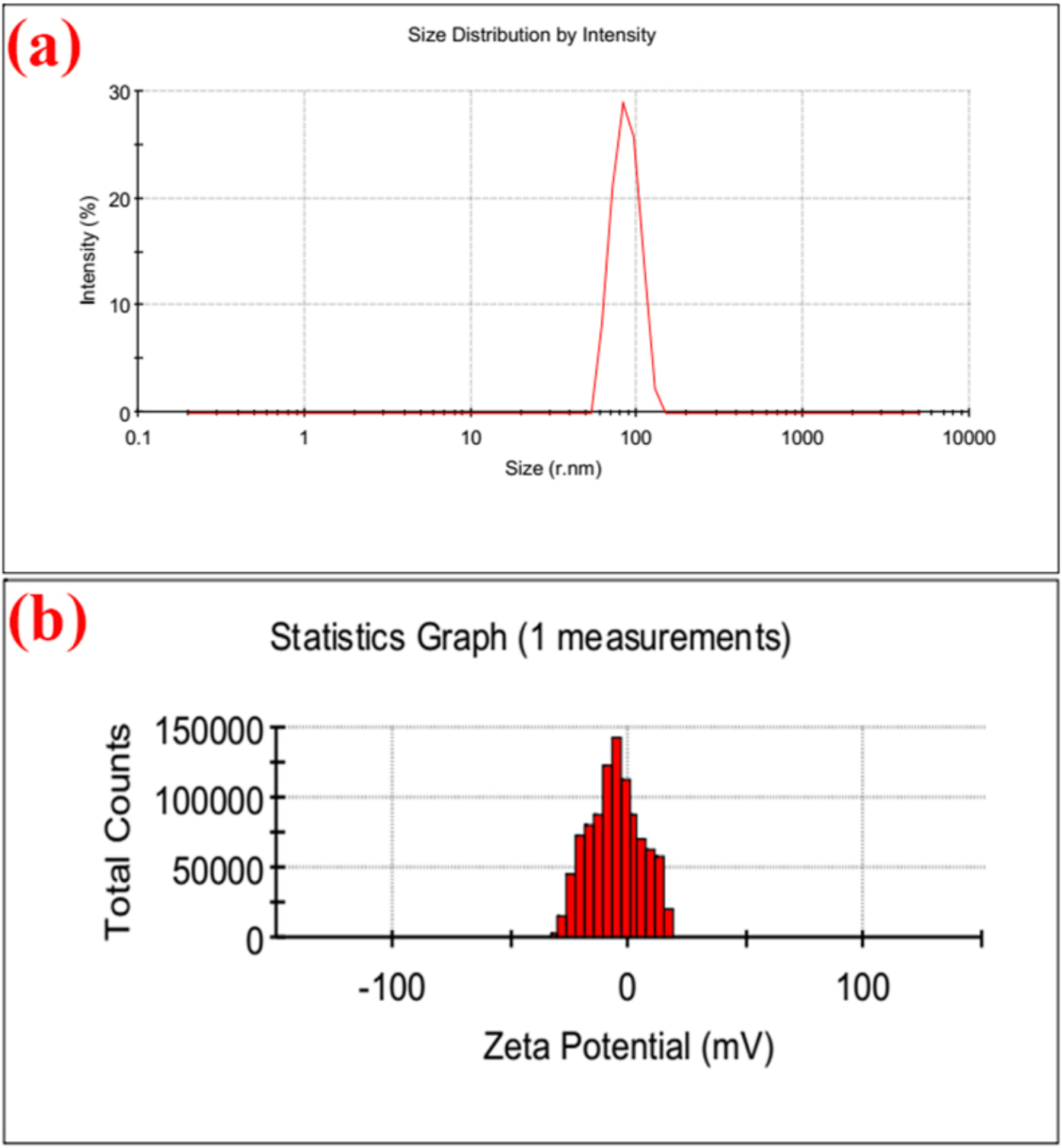

Figure 9

Particle size distribution obtained data from DLS (a) and Zeta potential measurements (b) of Cu nanoparticles in magnetic field equal to 10 mT and electrical potential equal to 50 volts

Supplementary Files

This is a list of supplementary files associated with this preprint. Click to download.

- Graphicalabstract.png